AIMS Mathematics, 10(11): 27898–27920.
DOI: 10.3934/math.20251225
Received: 09 October 2025
Revised: 19 November 2025
Accepted: 25 November 2025
Published: 28 November 2025

https://www.aimspress.com/journal/Math

Research article

Dynamics analysis and optimal control of a fractional-order SEAIQRM model with media effects

Wenli Huang, Ping Tong*, Jing Zhang, Qunjiao Zhang and Jie Liu

School of Mathematics and Statistics, Research Center of Nonlinear Science, Wuhan Textile University, Wuhan 430073, China

* **Correspondence:** Email: ptong@wtu.edu.cn.

Abstract: As a crucial research tool, epidemic models have played an important role in predicting disease progression. In this study, we delineated the full dynamics of epidemics by extending the susceptible–exposed–infectious–recovered (SEIR) model to include media effects (M), unascertained cases (A), and case isolation in a hospital (Q), generating a model that we called SEAIQRM. Dual time delays, aware susceptibles, and fractional order were also incorporated, synergistically enhancing the model's accuracy in depicting the real dynamic process of disease transmission. We calculated a specific expression for the basic reproduction number R_0, proved the existence and uniqueness of the model solution, and analyzed the local and global stability of two types of equilibrium points. To investigate the optimal control of the model, the sensitivity indices of the parameters in R_0 were computed, and vaccination rate and isolation rate were selected as control variables, exerting the strongest effects on R_0. Finally, the effectiveness of the model in illustrating and controlling the spread of infectious diseases is verified through numerical simulation. For a fractional order α in the interval [0.7, 0.9], the peak sizes of the asymptomatic (A) and symptomatic (I) compartments decreased significantly relative to the α=1 benchmark, corresponding to reductions of 32%–37% and 28%–33%, respectively. Implementing an optimal control strategy with vaccination (u = 0.4) and quarantine (q = 0.5) minimized implementation costs while achieving the most effective reduction in disease spread. The model can provide information regarding intervention timing in a setting with similar parameters. However, its use in the real-world requires calibration and validation.

Keywords: time delay; stability; optimal control; fractional-order differential equations; media effects; epidemic model
Mathematics Subject Classification: 34A08, 92D30, 49J20

1. Introduction

Since the 21st century, global public health has been confronted with security challenges posed by infectious diseases. Historically, the 1918 Spanish flu pandemic caused tens of millions of deaths with far-reaching effects. Subsequent threats, including SARS, COVID-19, and the H1N1, have further highlighted the urgency of addressing these issues. According to World Health Organization data [1] from 2022, over 10.2 million people worldwide die from epidemics each year, accounting for 18% of the total number of deaths. Epidemics not only pose threats to human life and health, but also result in substantial economic losses and exert profound effects on social structures.

Many mathematical models have been proposed, attempting to increase the understanding of the dynamical behavior of infectious diseases. Kermack and McKendrick [2] pioneered the classic compartmental model by dividing a population into three distinct groups: susceptible, infected, and removed. El-Shahed and El-Naby [3] developed a Susceptible-Vaccinated-Infectious-Recovered (SVIR) compartmental model to investigate the dynamics of childhood diseases and vaccine efficacy. The dynamics of HBV infection was modeled using differential equations [4], and also the epidemic dynamics of Ebola [5], dengue [6], and HIV [7].

Research has indicated that media effects are pivotal to infectious disease prevention and control. During the COVID-19 pandemic, mass media played a core role by disseminating key information, including updates on new infections and mortality rates, tracking of infected individuals' activity trajectories, detailed explanations of disease symptoms, and guidance on prevention and treatment. The public actively engaged in prevention and control, adopting measures such as mask-wearing, disinfectant use, and reduced visits to high-risk areas. These measures significantly curbed the spread of COVID-19 and other infectious diseases.

The profound effects of time delays on model dynamics and control have also been well-documented. Motivated by these insights, a variety of studies have extended classical epidemic models by integrating time delays and media effects through various analytical approaches. For example, Liu et al. [8] pioneered the integration of media coverage into epidemic modeling by proposing a media effect function to quantify its influence on disease outbreaks. Zaman et al. [9] developed an optimal control Susceptible-Infectious-Recovered (SIR) model with time delay, wherein control was implemented through the treatment of infected hosts. McCluskey [10] investigated an SIR model that incorporated distributed and discrete delays. Misra et al. [11] established a delayed model with media effects by accounting for the time delay in media campaign implementation. Wu et al. [12] enhanced an existing model by introducing two time delays and analyzed the existence of global solutions for the resulting time-delayed monostable epidemic model [13]. Kundu et al. [14] proposed a delayed epidemic model with saturated incidence and treatment functions, incorporating a delay to represent the temporary immunity period of recovered individuals. Greenhalgh et al. [15] improved model realism by introducing delays related to memory decay and media effects, analyzing equilibrium stability, and performing numerical simulations by using pneumonia as a case study. Kar et al. [16] embedded media effects into a SEIR framework by introducing a parameter M and directly transferring aware, susceptible individuals into the recovered compartment. Kabir et al. [17] formulated a reaction-diffusion model for media-influenced infectious diseases and examined the effects of key parameters including time delay, infection rate, and media effect. Feng et al. [18] constructed a COVID-19 model by incorporating media coverage and isolation measures, classifying susceptible individuals into aware

and unaware categories based on media reports. Li et al. [19] incorporated an exponential media function into a SIEM model with a dedicated media-effect variable to describe contact transmission rates, analyzing COVID-19 transmission patterns under dual media effects.

Although existing studies on media effects rely on integer-order models, the inherent memory and genetic traits of virus transmission are more accurately captured by fractional calculus. Furthermore, fractional-order models have an additional degree of freedom during parameter estimation, offering enhanced flexibility for data fitting [20]. This advantage has stimulated extensive research on fractional-order infectious disease dynamics.

Area et al. [5] concurrently analyzed classical and fractional SEIR models for Ebola, demonstrating that the fractional version provided better fit to real data. Singh et al. [21] formulated a fractional epidemiological model with non-singular kernel-based derivatives to characterize computer virus propagation and derived solutions via iterative methods. Sene [22] developed a delayed SIR epidemic model within the framework of Mittag-Leffler kernel-based fractional derivatives. Chen et al. [23] proposed a generalized fractional SEIAR model applicable to monomial and polynomial fractional differential equations, and introduced a reliable parameter estimation method that combined an improved hybrid Nelder–Mead simplex search with particle swarm optimization. Baleanu et al. [24] introduced a fractional model that incorporated isolation and quarantine mechanisms, established a generalized formulation, and derived corresponding stability criteria. In [25], Maji constructed and analyzed a fractional-order model that accounted for media influence on disease dynamics, finding that sufficiently strong media effects can induce stable oscillations in the system. Nisar et al. [26] developed a fractional-order model by employing multiple numerical techniques and tuning parameters associated with temporal fractional orders. Liang et al. [27] proposed a local fractional Vakhnenko–Parkes equation and applied the Mittag-Leffler function-based method to this equation for the first time. Wang [28] pioneered the construction of a fractal active low-pass filter on a Cantor set by using local fractional calculus. Hao et al. [29] proposed the next class of infectious disease models that incorporated presymptomatic and asymptomatic infections.

Motivated by advances in theoretical and applied epidemic modeling, the current study introduces a fractional-order model, called SEAIQRM, which incorporates dual time delays into media effects. To more accurately characterize real-world transmission scenarios, this study aims to develop a comprehensive, precise, and practically valuable theoretical framework. The proposed framework generalizes the classical integer-order models by incorporating key epidemiological features, including asymptomatic infections, quarantine measures, media effects, and stratification of susceptibles into aware and unaware populations, and it leverags the fractional-order parameter α as a pivotal regulator of memory intensity and dynamic evolution. This integration enables precise modulation of transmission rhythm, stability, threshold behavior, and control efficacy, precisely characterizing both the historical cumulative impact of viral transmission and the real-world delayed effects of intervention measures, and significantly strengthening the model's explanatory power and practical utility in real-world applications. The analysis establishes the basic reproduction number R_0 and identifies the disease-free equilibrium (DFE). Furthermore, it proves the existence and uniqueness of the endemic equilibrium while demonstrating the local asymptotic stability of the disease-free state. In addition, a sensitivity analysis of R_0 is conducted. Thereafter, control variables are selected to examine the model's optimal control. The theoretical findings are validated through numerical simulations, which also provide insights into system dynamics and optimal control policies.

The major contributions of the current study are summarized as follows: (1) Different from prior models [30, 31], this study presents an extended epidemic model, designated as SEAIQRM, which enhances the classical SEIR framework by incorporating media effects (M), unascertained infections (A), and hospital-based case isolation (Q). The model further refines the susceptible population by stratifying it into unaware (S_1) and aware (S_2) classes, thereby comprehensively capturing the full transmission-intervention-isolation continuum. Existing research has not yet incorporated all of these elements in a unified and comprehensive framework. (2) Compared with existing studies [32], this study presents the integrated framework that synergistically combines fractional calculus, dual time delays, and media effects. The approach leverages the memory dependence of fractional operators to capture the cumulative historical impact of virus transmission, while incorporating dual delays to realistically represent the non-instantaneous nature of media interventions in practice. (3) An optimal control problem is formulated for the proposed system that incorporates vaccination strategies, aiming to simultaneously minimize the total number of infections, maximize the size of the unaffected population, and reduce the overall intervention cost.

2. Preliminaries

Compared with other fractional derivatives, the Caputo fractional operator is adept at describing complex physical phenomena with memory and hereditary properties. This feature, coupled with its requirement for initial conditions in classical form, makes this operator particularly suitable for modeling physical systems. Consequently, the current study is based on Caputo type fractional derivative. Before the presentation and analysis of the model, the fractional integral and Caputo fractional derivative are introduced.

Definition 1. *The fractional integral of order $\alpha > 0$ for the appropriate function $f(t)$ can be described by the following expression [33]:*

$$I_t^{\alpha} f(t) = \frac{1}{\Gamma(\alpha)} \int_0^t (t-\zeta)^{\alpha-1} f(\zeta) d\zeta, t > 0, \tag{2.1}$$

where Γ represents the gamma function, which is used to extend the factorial to the domain of real and complex numbers.

Definition 2. *For the appropriate function $f(t)$, the Caputo fractional derivative of order α is defined as [33]:*

$${}^{C}D_t^{\alpha} f(t) = \frac{1}{\Gamma(n-\alpha)} \int_0^t (t-\zeta)^{n-\alpha-1} f^{(n)}(\zeta) d\zeta, t > 0, \tag{2.2}$$

where $n = \lceil \alpha \rceil + 1$; $\lceil \alpha \rceil$ denotes the smallest integer that is greater than or equal to α; and Γ represents the gamma function, which extends the factorial function to real and complex numbers.

3. Model formulation

In the SEAIQRM model introduced in the current study, the susceptible population is categorized into two groups: the unaware susceptible individuals S_1; and the aware susceptible individuals S_2. The members of the latter do not participate in disease transmission due to self-imposed isolation after

information uptake. Here, E refers to those in the latent infection stage who are infected but not yet infectious or symptomatic. A fraction of these individuals later progress to the symptomatic infectious class I, while the remainder enter the asymptomatic infectious class A. Both groups contribute to disease spread. The model further incorporates compartments for quarantined individuals Q, recovered individuals R, and media effects M.

In this model, direct inter-individual transmission is considered the primary route of disease spread. Presymptomatic infections are categorized as a form of asymptomatic infection, with a defined proportion assumed to develop symptomatic manifestations after a specific latency period. During the initial phase of an outbreak, increasing media coverage exposes initially unaware susceptible individuals to preventive health information, prompting their transition into an aware state. This heightened risk perception encourages the adoption of protective behavior, reducing disease transmission rates. However, disease-related information is not retained indefinitely, and thus, some aware individuals may revert into an unaware status once information dissemination wanes. To capture non-instantaneous transition along the causal pathway from information exposure to behavioral adaptation in real-world contexts, the model also incorporates two critical time delays: τ_1, which is a delay between receiving media information and developing self-protective awareness, and τ_2, which is a delay associated with the media processes of information acquisition and dissemination. The overall structure of the disease transmission process is illustrated in Figure 1.

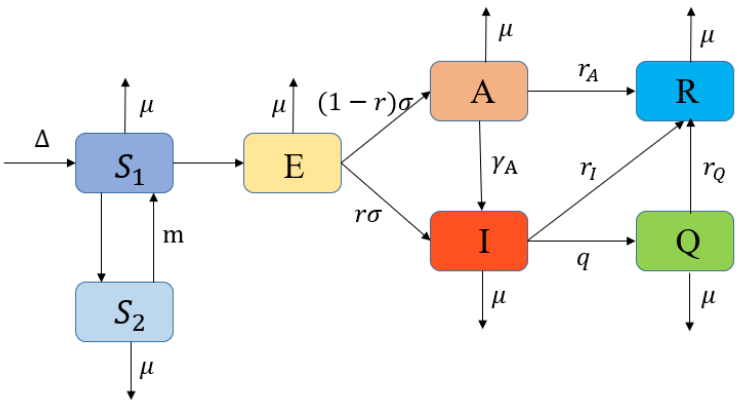

Figure 1. Disease transmission flow chart.

The epidemic process under consideration is described by the following system of fractional-order differential equations:

$$\begin{cases} {}^{C}D^{\alpha}S_1(t) = \Delta - \beta S_1 f(A, I) - \eta S_1 M(t-\tau_1) + mS_2 - \mu S_1, \\ {}^{C}D^{\alpha}S_2(t) = \eta S_1 M(t-\tau_1) - mS_2 - \mu S_2, \\ {}^{C}D^{\alpha}E(t) = \beta S_1 f(A, I) - \sigma E - \mu E, \\ {}^{C}D^{\alpha}A(t) = (1-r)\sigma E - \gamma_A A - r_A A - \mu A, \\ {}^{C}D^{\alpha}I(t) = r\sigma E + \gamma_A A - r_I I - qI - \mu I, \\ {}^{C}D^{\alpha}Q(t) = qI - r_Q Q - \mu Q, \\ {}^{C}D^{\alpha}R(t) = r_A A + r_I I + r_Q Q - \mu R, \\ {}^{C}D^{\alpha}M(t) = \xi[A(t-\tau_2) + I(t-\tau_2)] - \phi M. \end{cases} \tag{3.1}$$

The model parameters are described in Table 1.

Table 1. Description of model parameters.

Parameters	Descriptions	Value
Δ	Recruitment rate	0.05
β	Transmission rate of infected persons	0.41
ξ	Media effect impact	0.05
ϕ	Media effect dissemination loss	0.05
μ	mortality rate	0.05
η	Rate of dissemination of awareness	0.02
m	aware to unaware transfer rate	0.001
σ	Non-infectious to infectious conversion rate	0.35
r	Symp/asymp infection determination rate	0.23
γ_A	Asymptomatic to symptomatic conversion rate	0.42
r_A	Asymptomatic recovery rate	0.34
r_I	Symptomatic recovery rate	0.34
r_Q	Quarantine recovery rate	0.05
q	Symptomatic isolation rate	0.03
c	Undetermined to determined transmission ratio	0.55

4. Basic reproduction number and existence of equilibrium points

For any disease model, DFE represents a fundamental steady state that is crucial for determining whether an infection can invade a fully susceptible population.

The basic reproduction number R_0 serves as a threshold parameter that governs DFE stability. It is defined as the expected number of secondary infections that arise from a single typical infective individual in a completely susceptible population. The proposed model always admits DFE. Let $E = 0$ and $I = 0$. DFE is given by $X_0 = (\frac{\Delta}{\mu}, 0, 0, 0, 0, 0, 0, 0)$, which can be expressed in the following form:

$$\frac{dX}{dt} = \bar{F}(X) - \bar{G}(X), \tag{4.1}$$

where

$$\bar{F}(X) = \begin{bmatrix} \beta S_1 f \\ 0 \\ 0 \\ 0 \\ 0 \\ 0 \\ 0 \\ 0 \end{bmatrix}, \quad \bar{G}(X) = \begin{bmatrix} \sigma E + \mu E \\ -(1-r)\sigma E + \gamma_A A + r_A A + \mu A \\ -r\sigma E - \gamma_A A + r_I I + qI + \mu I \\ -\Delta + \beta S_1 f + \eta S_1 M(t-\tau_1) + \mu S_1 - mS_2 \\ -\eta S_1 M(t-\tau_1) + mS_2 + \mu S_2 \\ -qI + r_Q Q + \mu Q \\ -r_A A - r_I I - r_Q Q + \mu R \\ -\xi[A(t-\tau_2) + I(t-\tau_2)] + \phi M \end{bmatrix}. \tag{4.2}$$

Then, the Jacobian matrix of $\bar{F}(X)$ is

$$F(X) = \begin{bmatrix} 0 & \beta S_1(0) f_{A(0)} & \beta S_1(0) f_{I(0)} \\ 0 & 0 & 0 \\ 0 & 0 & 0 \end{bmatrix}, \tag{4.3}$$

and the Jacobi matrix of $\bar{G}(X)$ is

$$G(X) = \begin{bmatrix} \sigma + \mu & 0 & 0 \\ -(1-r)\sigma & \gamma_A + r_A + \mu & 0 \\ -r\sigma & -\gamma_A & r_I + q + \mu \end{bmatrix}. \tag{4.4}$$

Therefore, the spectral radius of the FG^{-1} matrix is the basic reproduction number of the model (3.1), i.e.,

$$R_0 = \frac{(1-r)\sigma\beta S_1(0) f_{A(0)}}{(\sigma+\mu)(\gamma_A + r_A + \mu)} + \frac{[\gamma_A(1-r)\sigma + r\sigma(\gamma_A + r_A + \mu)]\beta S_1(0) f_{I(0)}}{(\sigma+\mu)(\gamma_A + r_A + \mu)(r_I + q + \mu)}. \tag{4.5}$$

A rigorous proof of the solution's positivity precedes the examination of the model's local and global properties at the disease-free and endemic equilibria through R_0.

Theorem 1. *For any $t \geq 0$, the solution to the model (3.1) is non-negative.*

Proof. To establish the non-negativity of all solutions, the proof by contradiction method is used. Assume that a first time $t_0 \geq 0$ exists, at which one of the state variables becomes negative. Our goal is to demonstrate that such a situation is impossible. Without losing generality, suppose that $S_1(t_0) = 0$ and $S_1(t)$ becomes negative immediately after t_0. From the model equations, the derivative of S_1 at t_0 satisfies

$${}^C D^\alpha S_1(t_0) = \Delta - \beta S_1(t_0) f(A(t_0), I(t_0)) - \eta S_1(t_0) M(t_0 - \tau_1) + m S_2(t_0) - \mu S_1(t_0).$$

Given that $S_1(t_0) = 0$, the equation can be simplified into ${}^C D^\alpha S_1(t_0) = \Delta + m S_2(t_0)$.

Considering that $\Delta > 0$, then ${}^C D^\alpha S_1(t_0) \geq \Delta > 0$. This result indicates that $S_1(t)$ is non-decreasing at t_0, contradicting the assumption that it becomes negative. Through analogous reasoning, all the solutions of model (3.1) remain non-negative for all $t \geq 0$ cases. □

The model also admits an endemic equilibrium, representing a state of persistent infection within a population. The analysis of this equilibrium yields the following existence condition:

Theorem 2. *For model (3.1), if $R_0 < 1$, then the model only has the DFE point $X_0 = (\frac{\delta}{\mu}, 0, 0, 0, 0, 0, 0, 0)$. If $R_0 > 1$, then model (3.1) has a unique endemic equilibrium point $X^* = (S_1^*, S_2^*, E^*, A^*, I^*, Q^*, R^*, M^*)$, where all state variables satisfy $S_1^*, S_2^*, E^*, A^*, I^*, Q^*, R^*, M^* > 0$.*

Proof. The endemic equilibrium point X^* is defined by the condition that all fractional-order derivatives will vanish, i.e.,

$${}^C D^\alpha S_1(t) = {}^C D^\alpha S_2(t) = \ldots = {}^C D^\alpha M(t) = 0.$$

Setting the right side of model (3.1) to zero and solving the resulting algebraic system yields the following expression for endemic equilibrium:

$$\begin{cases} S_1^* = \frac{\Delta(m+\mu)}{\beta f(A^*,I^*)(m+\mu)+\mu(m+\mu)+\eta\xi(A^*+I^*)}, \ S_2^* = \frac{\eta S_1^*\xi[A^*+I^*]}{\phi(m+\mu)}, \ M^* = \frac{\xi[A^*+I^*]}{\phi}, \\ E^* = \frac{\beta\Delta(m+\mu)\sigma[c(1-r)p+rg+\gamma_A(1-r)]-\mu(m+\mu)gp(\sigma+\mu)}{\sigma(\sigma+\mu)[c(1-r)p+rg+\gamma_A(1-r)](m+\mu)+\eta\xi[(1-r)p+rg+\gamma_A(1-r)]}, \ A^* = \frac{(1-r)\sigma E^*}{g}, \\ I^* = \frac{[]r\sigma g+\gamma_A(1-r)\sigma]E^*}{gp}, \ Q^* = \frac{qI^*}{r_Q+\mu}, \ R^* = \frac{r_Q+\mu}{\mu[(r_AA^*+r_II^*)(r_Q+\mu)+r_Qq I^*]}, \end{cases}$$

where $g = \gamma_A + r_A + \mu$, $p = r_I + q + \mu$.

Existence: When $R_0 > 1$, the infection-driving terms in the numerator dominate the inhibitory effects in the denominator. This condition ensures the positivity of the right side of the equilibrium equation, implying the existence of a biologically meaningful solution $E^* > 0$. To formalize this finding, we define a continuous mapping $F : R^+ \to R^+$, as follows:

$$F(E^*) = \frac{\beta\Delta(m+\mu)\sigma[c(1-r)p+rg+\gamma_A(1-r)]-\mu(m+\mu)gp(\sigma+\mu)}{\sigma(\sigma+\mu)[c(1-r)p+rg+\gamma_A(1-r)](m+\mu)+\eta\xi[(1-r)p+rg+\gamma_A(1-r)]}.$$

Given the linear growth of $f(A^*, I^*)$ with respect to E^* and the condition $R_0 > 1$, a closed interval $[0, \overline{E}]$ exists, over which F forms self-mapping. In accordance with the Brouwer fixed-point theorem, this condition guarantees the existence of at least one positive solution $E^* > 0$ in the interval.

Uniqueness: As derived above, a nonlinear equation that concerns E^* is obtained. If the derivative of the right side of the equation with respect to E^* is negative, then the right side is strictly decreasing in E^*. By contrast, the left side E^* increases linearly. Within the domain of positive real numbers, such an equation admits at most one solution. Combined with the earlier existence result, this condition guarantees the uniqueness of the endemic equilibrium E^*.

Positivity of the solution: All state variables can be expressed as functions of $E^* > 0$. Given that all system parameters (Δ, μ, σ, ξ, ϕ, m, η) are positive and $R_0 > 1$ ensures the dominance of infection-sustaining terms, then S_1^*, S_2^*, E^*, A^*, I^*, Q^*, R^*, $M^* > 0$. This statement completes the proof of Theorem 2. □

Theorem 3. *If $R_0 < 1$, then the DFE point X_0 of model (3.1) is locally asymptotically stable. If $R_0 > 1$, then the DFE point X_0 of model (3.1) is unstable.*

Proof. The Jacobi matrix of the model at X_0 is

$$J(X_0) = \begin{pmatrix} -\mu & m & 0 & -\beta S_1(0) f_{A(0)} & -\beta S_1(0) f_{I(0)} & 0 & 0 & -\eta S_1(0) \\ 0 & -(m+\mu) & 0 & 0 & 0 & 0 & 0 & \eta S_1(0) \\ 0 & 0 & -(\sigma+\mu) & -\beta S_1(0) f_{A(0)} & \beta S_1(0) f_{I(0)} & 0 & 0 & 0 \\ 0 & 0 & (1-r)\sigma & -g & 0 & 0 & 0 & 0 \\ 0 & 0 & r\sigma & i & -p & 0 & 0 & 0 \\ 0 & 0 & 0 & 0 & q & -(r_Q+\mu) & 0 & 0 \\ 0 & 0 & 0 & r_A & r_I & r_Q & -\mu & 0 \\ 0 & 0 & 0 & \xi & \xi & 0 & 0 & -\phi \end{pmatrix},$$

where $g = \gamma_A + r_A + \mu$, $p = r_I + q + \mu$.

The characteristic equation that corresponds to $J(X_0)$ is

$$(\lambda+\mu)^2(\lambda+m+\mu)(\lambda+r_Q+\mu)(\lambda+\phi)T(\lambda) = 0, \tag{4.6}$$

and

$$\begin{aligned} T(\lambda) &= \begin{pmatrix} \lambda+\sigma+\mu & \beta S_1(0) f_{A(0)} & -\beta S_1(0) f_{I(0)} \\ -(1-r)\sigma & \lambda+\gamma_A+r_A+\mu & 0 \\ -r\sigma & -\gamma_A & \lambda+r_I+q+\mu \end{pmatrix} \\ &= (\lambda+\sigma+\mu)(\lambda+\gamma_A+r_A+\mu)(\lambda+r_I+q+\mu) \\ &- (1-r)\gamma_A\sigma\beta S_1(0) f_{I(0)} - r\sigma(\lambda+\gamma_A+r_A+\mu)\beta S_1(0) f_{I(0)} \\ &- (1-r)\sigma\beta S_1(0) f_{A(0)}(\lambda+r_I+q+\mu). \end{aligned} \tag{4.7}$$

Thus, the Jacobi matrix $J(X_0)$ has the following eigenvalues: $\lambda_1 = \lambda_2 = -\mu$, $\lambda_3 = -m-\mu$, $\lambda_4 = -r_Q-\mu$, $\lambda_5 = -\phi$.

Evidently, λ_1, λ_2, λ_3, λ_4, and λ_5 are negative real roots of the characteristic formula, Eq (4.6). The remaining eigenvalues of the characteristic equation have negative real parts, as proven below. Suppose that $\lambda = x + iy(x \geq 0)$ is an eigenvalue of the characteristic formula, Eq (4.7). Then, Eq (4.7) can be transformed into

$$\begin{aligned} 1 =& \frac{(1-r)\gamma_A\sigma\beta S_1(0) f_{I(0)}}{(\lambda+\sigma+\mu)(\lambda+\gamma_A+r_A+\mu)(\lambda+r_I+q+\mu)} + \frac{r\sigma\beta S_1(0) f_{I(0)}}{(\lambda+\sigma+\mu)(\lambda+r_I+q+\mu)} \\ &+ \frac{(1-r)\sigma\beta S_1(0) f_{A(0)}}{(\lambda+\sigma+\mu)(\lambda+\gamma_A+r_A+\mu)}. \end{aligned} \tag{4.8}$$

Substituting $\lambda = x + iy(x \geq 0)$ into Eq (4.8), we obtain

$$\begin{aligned} 1 =& \left|\frac{(1-r)\gamma_A\sigma\beta S_1(0) f_{I(0)}}{(x+iy+\sigma+\mu)(x+iy+g)(x+iy+p)} + \frac{r\sigma\beta S_1(0) f_{I(0)}}{(x+iy+\sigma+\mu)(x+iy+r_I+q+\mu)}\right. \\ &\left. + \frac{(1-r)\sigma\beta S_1(0) f_{A(0)}}{(x+iy+\sigma+\mu)(x+iy+\gamma_A+r_A+\mu)}\right| \\ =& \left|\frac{(1-r)i\sigma\beta S_1(0) f_{I(0)}}{(\sqrt{(x+\sigma+\mu)^2)+y^2})(\sqrt{(x+g)^2)+y^2})(\sqrt{(x+p)^2)+y^2})}\right| \\ &+ \left|\frac{r\sigma\beta S_1(0) f_{I(0)}}{(\sqrt{(x+\sigma+\mu)^2)+y^2})(\sqrt{(x+r_I+q+\mu)^2)+y^2})}\right| + \left|\frac{(1-r)\sigma\beta S_1(0) f_{A(0)}}{(\sqrt{(x+\sigma+\mu)^2)+y^2})(\sqrt{(x+p)^2)+y^2})}\right| \\ <& \frac{(1-r)i\sigma\beta S_1(0) f_{I(0)}}{(\sigma+\mu)(\gamma_A+r_A+\mu)p} + \frac{r\sigma\beta S_1(0) f_{I(0)}}{(\sigma+\mu)(r_I+q+\mu)} + \frac{(1-r)\sigma\beta S_1(0) f_{A(0)}}{(\sigma+\mu)(\gamma_A+r_A+\mu)} \\ =& R_0. \end{aligned}$$

This result contradicts the initial assumption that $R_0 < 1$. Hence, all the eigenvalues of the characteristic formula, Eq (4.7), have negative real parts. Thus, DFE point X_0 is locally asymptotically stable when $R_0 < 1$. This statement completes the proof of Theorem 3. □

Theorem 4. *The endemic equilibrium point X^* of model (3.1) is locally asymptotically stable if $R_0 > 1$. If $R_0 < 1$, then the endemic equilibrium point X^* of model (3.1) is unstable.*

Proof. The Jacobian matrix of the model at the endemic equilibrium point X^* is

$$J(X^*) = \begin{pmatrix} -\mu & m & 0 & -\beta S_1^* f_{A^*} & -\beta S_1^* f_{I^*} & 0 & 0 & -\eta S_1^* \\ \eta M^* & -(\alpha+\mu) & 0 & 0 & 0 & 0 & 0 & \eta S_1^* \\ \beta f(A^*, I^*) & 0 & -(\sigma+\mu) & -\beta S_1^* f_{A^*} & \beta S_1^* f_{I^*} & 0 & 0 & 0 \\ 0 & 0 & (1-r)\sigma & -g & 0 & 0 & 0 & 0 \\ 0 & 0 & r\sigma & i & -p & 0 & 0 & 0 \\ 0 & 0 & 0 & 0 & q & -(r_Q+\mu) & 0 & 0 \\ 0 & 0 & 0 & r_A & r_I & r_Q & -\mu & 0 \\ 0 & 0 & 0 & \xi & \xi & 0 & 0 & -\phi \end{pmatrix},$$

where $g = \gamma_A + r_A + \mu$, $p = r_I + q + \mu$.

Thus, the characteristic equation that corresponds to $J(X^*)$ is

$$(\lambda+\mu)(\lambda+r_Q+\mu)[(-m\eta M^*)L_4[L_1L_2L_3 - (1-r)\gamma_A\sigma\beta S_1^* f_{I^*} + r\sigma\beta S_1^* f_{I^*}L_2 - (1-r)\sigma\beta S_1^* f_{I^*}L_3] + (-m\eta S_1^*\beta f(A^*, I^*))[-(1-r)\sigma\gamma_A\xi - \xi(1-r)\sigma L_3 - r\sigma\xi L_2]] = 0.$$

To simplify the expression, let $L_1 = \lambda + \sigma + \mu$, $L_2 = \lambda + \gamma_A + r_A + \mu$, $L_3 = \lambda + r_I + q + \mu$, $L_4 = \lambda + \phi$.

From an argument that is analogous to the proof of Theorem 1, all the eigenvalues of the characteristic equation have negative real parts when $R_0 > 1$. Consequently, endemic equilibrium X^* is locally asymptotically stable. This finding completes the proof of Theorem 4. □

Theorem 5. *If $R_0 > 1$, then model (3.1) has a unique endemic equilibrium point X^* that is globally asymptotically stable.*

Proof. First, the Lyapunov function is defined as

$$^C D^\alpha V = (1 - \frac{S_1^*}{S_1})^C D^\alpha S_1 + ... + (1 - \frac{M^*}{M})^C D^\alpha M,$$

where S_1^*, S_2^*, E^*, A^*, I^*, and M^* denote the components of the endemic equilibrium X^*. This function quantifies the energy associated with a system's deviation from its steady state by evaluating the logarithmic divergence of each state variable from the equilibrium.

By applying the chain rule for Caputo fractional derivatives, we compute $^C D^\alpha V$ along the solution trajectories of model (3.1) as follows:

$$^C D^\alpha V = (1 - \frac{S_1^*}{S_1})^C D^\alpha S_1 + ... + (1 - \frac{M^*}{M})^C D^\alpha M.$$

Considering $S_1(t)$ as an illustrative case, its substitution into the model equation yields

$$^C D^\alpha S_1 = \Delta - \beta S_1 f(A, I) - \eta S_1 M(t-\tau_1) - \mu S_1 + m S_2.$$

At endemic equilibrium X^*, the identity $\Delta = \beta S_1^* f(A^*, I^*) + \eta S_1^* M^*(t-\tau_1) + \mu S_1^* - m S_2^*$ is maintained. Substituting this relation and simplifying the result leads to

$$(1 - \frac{S_1^*}{S_1})[-\beta(S_1 f(A, I) - S_1^* f(A^*, I^*)) - \eta(S_1 M(t-\tau_1) - S_1^* M^*) + m(S_2 - S_2^*) - \mu(S_1 - S_1^*)].$$

Applying the logarithmic inequality $x - 1 - \ln x \geq 0$, we transform cross terms into square terms. Under the condition $R_0 > 1$, the structure of the basic reproduction number (4.5) reveals that the infection term $\beta S_1^* f(A^*, I^*)$ dominates over the suppression terms, such as natural mortality μ and media effect $\eta\xi$. This dominance allows the infection term to be decomposed as follows:

$$-\beta(S_1 f(A, I) - S_1^* f(A^*, I^*)) = -\beta S_1^* f(A^*, I^*)(\frac{S_1 f(A, I)}{S_1^* f(A^*, I^*)} - 1 - \ln \frac{S_1 f(A, I)}{S_1^* f(A^*, I^*)}) \leq 0.$$

When $R_0 > 1$, the magnitude of the numerator $\beta S_1^* f(A^*, I^*)$ guarantees its dominance in governing the negativity of the derivative. Similarly,

$$-\eta(S_1 M(t - \tau_1) - S_1^* M^*) = -\eta S_1^* M^*(\frac{S_1 M(t - \tau_1)}{S_1^* M^*} - 1 - \ln \frac{S_1 M(t - \tau_1)}{S_1^* M^*}) \leq 0.$$

By extending analogous analysis to all system variables, a conclusion can be drawn that ${}^C D^\alpha V \leq 0$, with equality holding if and only if $S_1 = S_1^*, \ldots, M = M^*$.

In accordance with the LaSalle invariance principle for fractional-order systems, all system trajectories eventually converge to the largest invariant set $M = \{x \in \mathbb{R} | {}^C D^\alpha V = 0\}$. Based on the preceding analysis, this set consists solely of the endemic equilibrium X^*. Consequently, all solutions converge globally to X^*. Moreover, the delayed state variables are reduced to constants at the equilibrium, implying that time delays do not affect the sign definiteness of the fractional derivative. This finding completes the proof of Theorem 5. □

5. Sensitivity analysis

A sensitivity analysis reveals the importance of each parameter to disease transmission. It provides information about the design of effective and cost-efficient strategies for disease control and prevention. By examining how variations in the parameters of R_0 influence its value, the sensitivity analysis identifies the most influential parameters and quantifies their contributions to disease spread. This knowledge allows policymakers to adjust critical parameters strategically, steering R_0 toward 1 to reduce infection prevalence and curb transmission. Consider the function $f(A, I) = cA + I$, where c denotes the transmission rate ratio between asymptomatic and symptomatic infected individuals. The sensitivity indices of the parameters in R_0 are computed using the normalized forward sensitivity index method described in [34]. The corresponding formula is given in Eq (5.1):

$$\varphi_\rho{}^{R_0} = \frac{\partial R_0}{\partial \rho} \frac{\rho}{R_0}. \tag{5.1}$$

The sensitivity indices of the parameters ρ in R_0 are computed using Eq (5.1), as described below:

$$\varphi_{\beta}^{R_0} = 1, \varphi_{\gamma_A}^{R_0} = \frac{(1-r\sigma)\gamma_A L_2 - \gamma_A \sigma c L_1 (1-r) - {\gamma_A}^2)(1-r)\sigma}{L_2 \sigma (1-r)(cL_1 + \gamma_A) + r\sigma {L_2}^2},$$

$$\varphi_{S_1(0)}^{R_0} = 1, \varphi_{\sigma}^{R_0} = \frac{\mu}{(\sigma+\mu)\sigma}, \varphi_{r_A}^{R_0} = \frac{-r_A[(1-r)cL_1 + \gamma_A(1-r)]}{(1-r)cL_1 L_2 + [\gamma_A(1-r) + rL_2]L_2},$$

$$\varphi_{r_I}^{R_0} = \frac{-r_I[\gamma_A(1-r) + rL_2]}{(1-r)c{L_1}^2 + [\gamma_A(1-r) + rL_2]L_1}, \varphi_{r}^{R_0} = \frac{-cL_1 - \gamma_A + L_2}{(1-r)cL_1 + \gamma_A(1-r) + rL_2},$$

$$\varphi_{q}^{R_0} = \frac{-q\gamma_A(1-r) + qrL_2}{c(1-r){L_3}^2 + L_3[\gamma_A(1-r) + rL_2]}, \varphi_{c}^{R_0} = \frac{c(1-r)}{c(1-r)L_1 + \gamma_A(1-r) + rL_2},$$

$$\varphi_{\mu}^{R_0} = \frac{-[(1-r)c + r]L_1{L_2}^2 - [(1-r)c - r]L_3{L_2}^2}{L_1 L_2 L_3[(1-r)cL_1 + \gamma_A(1-r) + rL_2]} - \frac{\gamma_A(1-r)(L_1L_2 + L_2L_3 + L_1L_3)}{L_1L_2L_3[(1-r)cL_1 + \gamma_A(1-r) + rL_2]},$$

where $L_1 = r_I + q + \mu$, $L_2 = \sigma + \mu$, and $L_3 = \gamma_A + r_A + \mu$.

The sign of the sensitivity index reflects the nature of the correlation between a parameter and R_0: A negative value denotes an inverse relationship, while a positive value indicates a positive association. The numerical results identify the isolation rate q as the most influential parameter on R_0. Consequently, effective intervention strategies should prioritize enhancing the isolation and management of infected individuals and minimizing contact between susceptible and infected populations. Such measures disrupt transmission pathways and reduce viral dissemination efficiency. The influence of each parameter on R_0 is visually summarized in Figure 2.

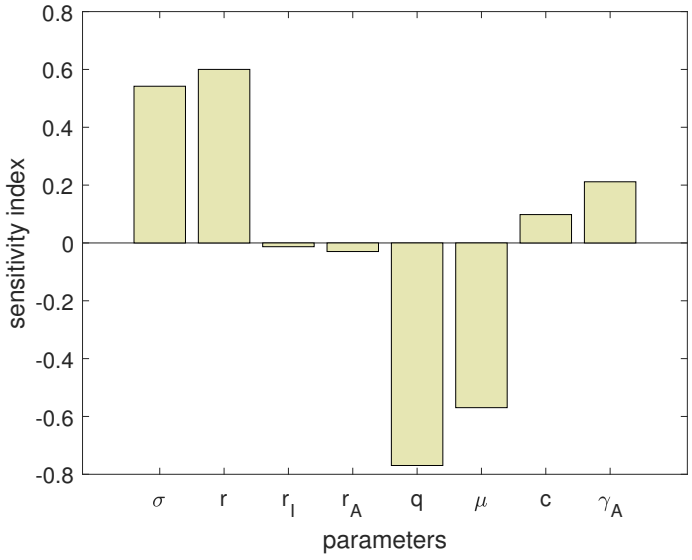

Figure 2. Relative impact of model parameters on R_0.

6. Optimal control

6.1. Formulation of the optimal control problem

In epidemiological modeling, optimal control theory provides a rigorous framework for designing effective public health interventions. The central aim is to achieve disease containment while

systematically evaluating the cost-effectiveness and practical feasibility of control measures. In the current study, the vaccination rate and isolation rate of symptomatic infected individuals are selected as control variables. The objective function, which incorporates infection prevalence, control costs, and disease duration, is formulated as follows:

$$J = \int_0^T (w_1 A + w_2 I + \frac{1}{2} w_3 (u(t))^2 + \frac{1}{2} w_4 (q(t))^2 + \frac{1}{2} w_5 d^2) dx. \tag{6.1}$$

Here, w_1, w_2, w_3, w_4, and w_5 represent the corresponding weighting coefficients, all of which are positive real numbers. These coefficients balance the relative importance of disease transmission scale and control costs within the objective function. The control variables $u(t)$ and $q(t)$ denote time-dependent vaccination and isolation rates, respectively, while d represents the cumulative number of deaths. The corresponding control constraints are given by

$$U_{ad} = \{(u, q) | 0 < u(t) < 1, 0 < q < 1\}. \tag{6.2}$$

Upon incorporating control variables $u(t)$ and $q(t)$ into system (3.1), the resulting controlled system dynamics are governed by the following equations:

$$\begin{cases} {}^C D^\alpha S_1(t) = \Delta - \beta S_1 f - \eta S_1 M(t - \tau_1) + m S_2 - \mu S_1 - u(t) S_1, \\ {}^C D^\alpha S_2(t) = \eta S_1 M(t - \tau_1) - m S_2 - \mu S_2 - u(t) S_2, \\ {}^C D^\alpha E(t) = \beta S_1 f(A, I) - \sigma E - \mu E, \\ {}^C D^\alpha A(t) = (1 - r)\sigma E - \gamma_A A - r_A A - \mu A, \\ {}^C D^\alpha I(t) = r\sigma E + \gamma_A A - r_I I - q(t) I - \mu I, \\ {}^C D^\alpha Q(t) = q(t) I - r_Q Q - \mu Q, \\ {}^C D^\alpha R(t) = r_A A + r_I I + r_Q Q - \mu R + u(t) S_1 + u(t) S_2, \\ {}^C D^\alpha M(t) = \xi [A(t - \tau_2) + I(t - \tau_2)] - \phi M. \end{cases} \tag{6.3}$$

The optimal control objective of the current study is to determine the pair $(u^*, q^*) \in u_{ad}$ that satisfies

$$J(u, q) = \inf_{(u^*, q^*) \in u_{\text{ad}}} J(u^*, q^*). \tag{6.4}$$

6.2. Existence and uniqueness of optimal control

Theorem 6. *An optimal control for the control problem (6.1)–(6.4) exists.*

Proof. To prove the existence of optimal control by using Theorem 4.1 from [35], verifying the following conditions is sufficient:

(1) The set of admissible states is non-empty.

(2) The control constraint set U_{ad} is convex and closed.

(3) The right side of the control system (6.3) is bounded by a linear function of the state and control variables.

(4) The integrand of the objective function

$$L(A, I, u, q, d) = w_1 A + w_2 I + \frac{1}{2} w_3 (u(t))^2 + \frac{1}{2} w_4 (q(t))^2 + \frac{1}{2} w_5 d^2$$

is convex on U_{ad}.

(5) Constants $h_1, h_2 > 0$ exist, such that the integrand satisfies

$$w_1A + w_2I + \frac{1}{2}w_3(u(t))^2 + \frac{1}{2}w_4(q(t))^2 + \frac{1}{2}w_5d^2 \geq h_1|u| + h_2|q|.$$

Then, we prove each of the five conditions above:

(1) In accordance with the proof of existence and uniqueness of the solution to the state system, the set of admissible states is non-empty.

(2) For any $U_1 = (u_1, q_1)$, $U_2 = (u_2, q_2) \in U_{ad}$, and any $\lambda \in [0, 1]$, let $U_3 = \lambda(u_1, q_1) + (1-\lambda)(u_2, q_2)$. Given that $0 \leq u_i \leq 1$, $0 \leq q_i \leq 1$ $(i = 1, 2)$, $0 \leq \lambda u_1 + (1-\lambda)u_2 \leq 1$, and $0 \leq \lambda q_1 + (1-\lambda)q_2 \leq 1$ hold. Thus, $U_3 \in U_{ad}$, implying that U_{ad} is a convex set. In addition, for any convergent sequence $U_n \in U_{ad}$, $\lim\limits_{n\to\infty} u_n = u$, and $\lim\limits_{n\to\infty} q_n = q$. Given that $0 \leq u_n \leq 1$ and $0 \leq q_n \leq 1$, then $0 \leq x \leq 1$ and $0 \leq q \leq 1$. Thus U_{ad} is a closed set.

(3) By disregarding the negative terms in state system (6.3) and given $0 \leq u \leq 1$ and $0 \leq q \leq 1$, then

$$\begin{pmatrix} {}^CD^\alpha S_1(t) \\ {}^CD^\alpha S_2(t) \\ {}^CD^\alpha E(t) \\ {}^CD^\alpha A(t) \\ {}^CD^\alpha I(t) \\ {}^CD^\alpha Q(t) \\ {}^CD^\alpha R(t) \end{pmatrix} < \begin{pmatrix} 0 & \alpha & 0 & 0 & 0 & 0 & 0 \\ \eta M & 0 & 0 & 0 & 0 & 0 & 0 \\ \beta f(A, I) & 0 & 0 & 0 & 0 & 0 & 0 \\ 0 & 0 & (1-r)\sigma & 0 & 0 & 0 & 0 \\ 0 & 0 & r\sigma & \gamma_A & 0 & 0 & 0 \\ 0 & 0 & 0 & 0 & 1 & 0 & 0 \\ 1 & 1 & 0 & r_A & r_I & r_Q & 0 \end{pmatrix} + \begin{pmatrix} \Delta \\ 0 \\ 0 \\ 0 \\ 0 \\ 0 \\ 0 \end{pmatrix}. \tag{6.5}$$

Thus, Condition 3 holds.

(4) Evidently, $L(A, I, u, q, d) = w_1A + w_2I + \frac{1}{2}w_3(u(t))^2 + \frac{1}{2}w_4(q(t))^2 + \frac{1}{2}w_5d^2$ is convex with respect to control variables u and q on U_{ad}.

(5) By taking

$$h_1 = \frac{1}{2}w_3(\min(1, \sqrt{w_3}, \sqrt{w_4})),$$

and

$$h_2 = \frac{1}{2}w_4(\min(1, \sqrt{w_3}, \sqrt{w_4})),$$

we obtain the inequality $w_1A + w_2I + \frac{1}{2}w_3(u(t))^2 + \frac{1}{2}w_4(q(t))^2 + \frac{1}{2}w_5d^2 \geq h_1|u| + h_2|q|$, which verifies that Condition 5 is satisfied. □

6.3. Optimality requirement

On the basis of the objective function, the Hamiltonian function H is constructed as follows:

$$H = L + \lambda_1^C D^\alpha S_1(t) + \lambda_2^C D^\alpha S_2(t) + \lambda_3^C D^\alpha E(t) + \lambda_4^C D^\alpha A(t) + \lambda_5^C D^\alpha I(t) + \lambda_6^C D^\alpha Q(t) + \lambda_7^C D^\alpha R(t), \tag{6.6}$$

where λ_1, λ_2, λ_3, λ_4, λ_5, λ_6, and λ_7 are accompanying variables.

Theorem 7. *Let $(S_1^*,\ S_2^*,\ E^*,\ A^*,\ I^*,\ Q^*,\ R^*,\ u^*,\ q^*)$ be the optimal pair of the optimal control problem (6.1)–(6.4). Then, the accompanying variables $\lambda_1,\ \lambda_2,\ \lambda_3,\ \lambda_4,\ \lambda_5,\ \lambda_6$, and λ_7 are satisfied*

$$\begin{cases} {}^CD^\alpha\lambda_1 = & \lambda_1(\beta f(A^*,I^*)+\mu+u^*)-\lambda_3\beta f(A,I)-\lambda_7u^*,\\ {}^CD^\alpha\lambda_2 = & -\lambda_1 m+\lambda_2(m+\mu+u^*)-\lambda_7u^*,\\ {}^CD^\alpha\lambda_3 = & \lambda_3\mu-\lambda_4(1-r)\sigma-\lambda_5r\sigma,\\ {}^CD^\alpha\lambda_4 = & -w_1+\lambda_1\beta S_1f_A(A^*,I^*)-\lambda_3\beta S_1f_A(A^*,I^*)+\lambda_4(\gamma_A+r_A+\mu)-\lambda_5\gamma_A-\lambda_7r_A,\\ {}^CD^\alpha\lambda_5 = & -w_2+\lambda_1\beta S_1f_I(A^*,I^*)-\lambda_3\beta S_1f_I(A^*,I^*)+\lambda_5(r_I+q^*+\mu)-\lambda_6q^*-\lambda_7r_I,\\ {}^CD^\alpha\lambda_6 = & \lambda_6(r_Q+\mu)-\lambda_7r_Q,\\ {}^CD^\alpha\lambda_7 = & -\lambda_7\mu. \end{cases} \tag{6.7}$$

With the following horizontal conditions:

$$\lambda_1=\lambda_2=\lambda_3=\lambda_4=\lambda_5=\lambda_6=\lambda_7=0. \tag{6.8}$$

Furthermore, optimal control can be expressed as

$$\begin{cases} u^* = min(1,max(0,u(t))),\\ q^* = min(1,max(0,q(t))). \end{cases} \tag{6.9}$$

Proof. Substituting control system (6.3) into the Hamiltonian function (6.6) yields

$$\begin{aligned} H(t) =& w_1A+w_2I+\frac{1}{2}w_3(u(t))^2+\frac{1}{2}w_4(q(t))^2+\frac{1}{2}w_5d^2\\ &+\lambda_1[\Delta-\beta S_1f(A,I)-\eta S_1M(t-\tau_1)+mS_2-\mu S_1-u(t)S_1]\\ &+\lambda_2[\eta S_1M(t-\tau_1)-mS_2-\mu S_2-u(t)S_2]+\lambda_3[\beta S_1f(A,I)-\sigma E-\mu E]\\ &+\lambda_4[(1-r)\sigma E-\gamma_AA-r_AA-\mu A]+\lambda_5[r\sigma E+\gamma_AA-r_II-q(t)I-\mu I]\\ &+\lambda_6[q(t)I-r_QQ-\mu Q]+\lambda_7[r_AA+r_II+r_QQ-\mu R+u(t)S+u(t)C]. \end{aligned} \tag{6.10}$$

For any $t\in[0,T]$, the application of Pontryagin's minimum principle yields the following necessary conditions:

$$\begin{cases} {}^CD^\alpha\lambda_1 = & -\frac{\partial H}{\partial S_1}=\lambda_1(\beta f(A^*,I^*)+\mu+u^*)-\lambda_3\beta f(A,I)-\lambda_7u^*,\\ {}^CD^\alpha\lambda_2 = & -\frac{\partial H}{\partial S_2}=-\lambda_1m+\lambda_2(m+\mu+u^*)-\lambda_7u^*,\\ {}^CD^\alpha\lambda_3 = & -\frac{\partial H}{\partial E}=\lambda_3\mu-\lambda_4(1-r)\sigma-\lambda_5r\sigma,\\ {}^CD^\alpha\lambda_4 = & -\frac{\partial H}{\partial A}=-w_1+\lambda_1\beta S_1f_A(A^*,I^*)-\lambda_3\beta S_1f_A(A^*,I^*)+\lambda_4(\gamma_A+r_A+\mu)-\lambda_5\gamma_A-\lambda_7r_A,\\ {}^CD^\alpha\lambda_5 = & -\frac{\partial H}{\partial I}=-w_2+\lambda_1\beta S_1f_I(A^*,I^*)-\lambda_3\beta S_1f_I(A^*,I^*)+\lambda_5(r_I+q^*+\mu)-\lambda_6q^*-\lambda_7r_I,\\ {}^CD^\alpha\lambda_6 = & -\frac{\partial H}{\partial Q}=\lambda_6(r_Q+\mu)-\lambda_7r_Q,\\ {}^CD^\alpha\lambda_7 = & -\frac{\partial H}{\partial R}=-\lambda_7\mu. \end{cases} \tag{6.11}$$

Furthermore, under optimal control conditions with $u=u^*$ and $q=q^*$, $\frac{dH}{du}=0$ and $\frac{dH}{dq}=0$ hold, leading to the following expressions:

$$\begin{cases} u(t)=\frac{(\lambda_1-\lambda_7)S_1+(\lambda_2-\lambda_7)S_2}{w_3},\\ q(t)=\frac{(\lambda_5-\lambda_6)I}{w_4}. \end{cases} \tag{6.12}$$

Moreover, the following can be derived from the control constraints:

$$\begin{cases} u^* = min(1, max(0, u(t))), \\ q^* = min(1, max(0, q(t))). \end{cases} \tag{6.13}$$

Thus, the proof of Theorem 7 is completed. □

7. Numerical simulation

This section investigates the solution influencing factors of model (3.1) and the optimal control characteristics of model (6.3) through numerical simulations. The parameter values adopted in our simulations are derived from [29].

7.1. Numerical simulation and discussion of model dynamics

In model (3.1), the transmission function is defined as $f(A, I) = cA + I$, where c denotes the relative transmission rate ratio between undetected and detected infections. Moreover,

$$(S_1(0), S_2(0), E(0), A(0), I(0), Q(0), R(0), M(0))^T = (0.8, 0, 0.03, 0.07, 0.1, 0, 0, 0)^T,$$

with the remaining parameters summarized in Table 1, we further examine the influences of fractional order, media effect, media dissipation rate, and time delays on system dynamics, as visualized in Figures 3–6.

Figure 3 displays the temporal evolution of asymptomatic infections A under varying parameter configurations. The results demonstrate the substantial influences of media effect intensity and information dissipation rate on asymptomatic transmission dynamics. Notably, the prevalence of asymptomatic infections exhibits a gradual decline with increasing fractional order. With the incorporation of media-related time delays, the prevalence of asymptomatic infections progressively decreases as delay duration extends. These findings indicate that fractional order governs the decay rate of A by modulating a system's memory effects. Meanwhile, enhanced media effect ξ suppresses disease transmission, while elevated dissipation rates ϕ diminish its effectiveness, underscoring the need to balance information coverage with persistence. Furthermore, delays in intervention implementation τ_2 prolong the transmission cycle of A, mathematically validating the essential principle of "early detection, early isolation" in epidemic control.

Figure 4 illustrates the temporal dynamics of symptomatically infected individuals I under various parameter conditions. The results demonstrate a declining trend in I with increasing fractional order, highlighting the memory-dependent regulatory role of fractional calculus in shaping symptomatic infection dynamics. However, the influence of media effect and its loss are significantly negatively correlated with the cumulative scale of I. These findings reinforce the notion that intensified public health communication can effectively compress the epidemiological timeline. Furthermore, prolonged time delays τ_2 lead to a gradual increase in symptomatic infections I. To minimize the prevalence of symptomatic cases, establishing an emergency response mechanism with $\tau_2 < 10$ days is essential.

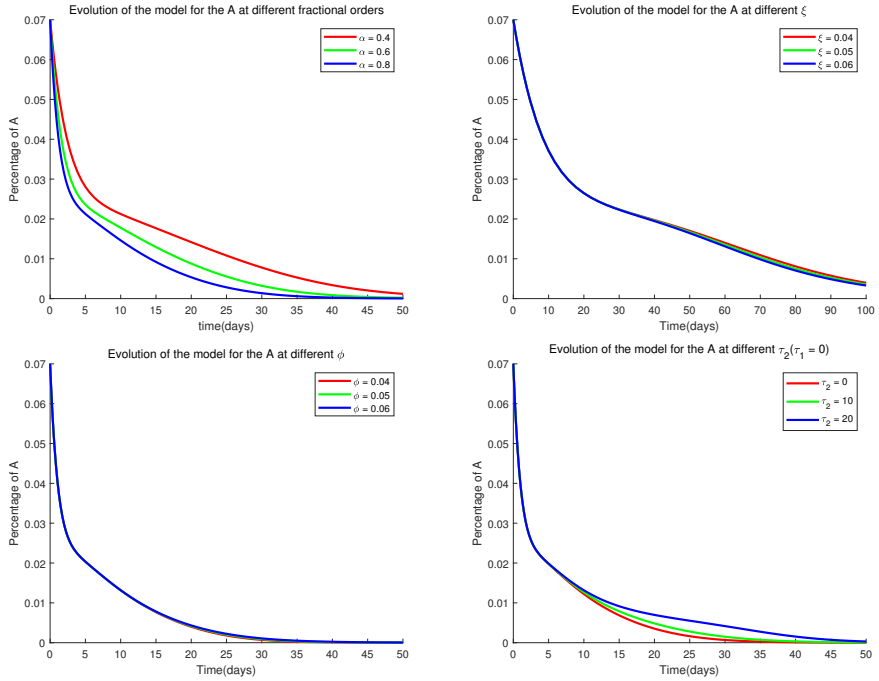

Figure 3. Evolution of asymptomatic infections A under varying: (a) fractional order $\alpha = 0.4, 0.6, 0.8$, (b) media impact $\xi = 0.004, 0.005, 0.006$, (c) media decay $\phi = 0.04, 0.05, 0.06$, (d) delay $\tau_2 = 0, 10, 20$ days.

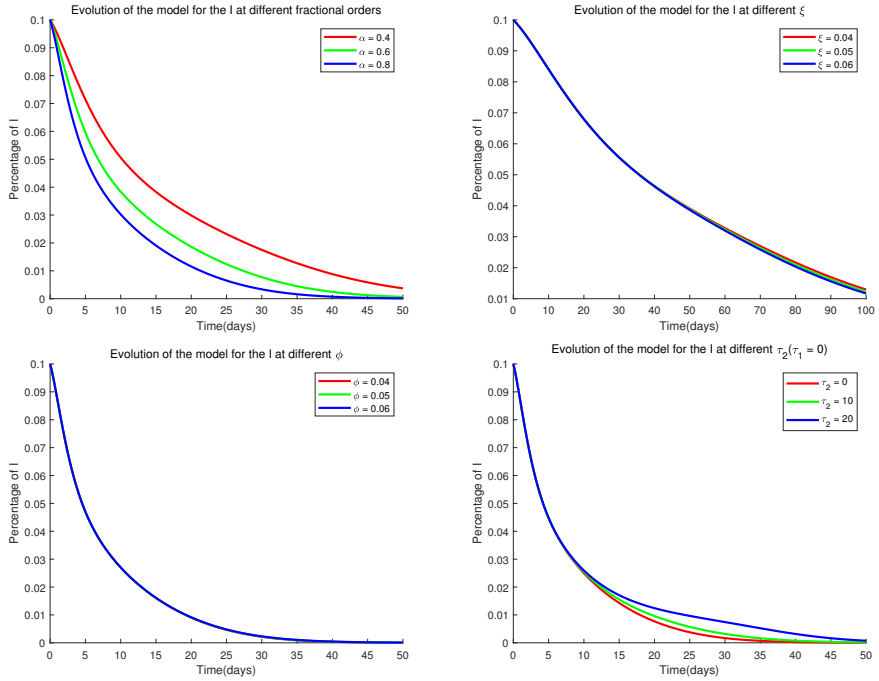

Figure 4. Evolution of symptomatic infections I under varying: (a) fractional order $\alpha = 0.4$, 0.6, 0.8, (b) media impact $\xi = 0.004, 0.005, 0.006$, (c) media decay $\phi = 0.04, 0.05, 0.06$, (d) delay $\tau_2 = 0, 10, 20$ days.

Figure 5 depicts the evolution of unaware susceptible individuals S_1 under different parameter settings. As α increases from 0.4 to 0.8, the decay rate of S_1 accelerates significantly. This phenomenon can be explained by the fact that a higher α reduces the integral weight of historical states, enhancing a system's sensitivity to current media interventions. Moreover, with the strengthening of media influence, the number of unaware susceptible individuals gradually decreases, while the number of aware individuals increases. Thus, increasing ξ can promote the cognitive transition of unaware susceptible individuals. A notable shift in S_1 is observed as media effect dissipation rate ϕ increases from 0.04 to 0.06. Therefore, maintaining ϕ below 0.05 is advisable to sustain the effectiveness of interventions. In addition, time delay should be carefully controlled to manage the size of S_1. The synergistic optimization of fractional-order parameters, media effects, and time-delayed control facilitates the effective conversion of unaware susceptible individuals, establishing a quantitative dynamic basis for public health information intervention strategies.

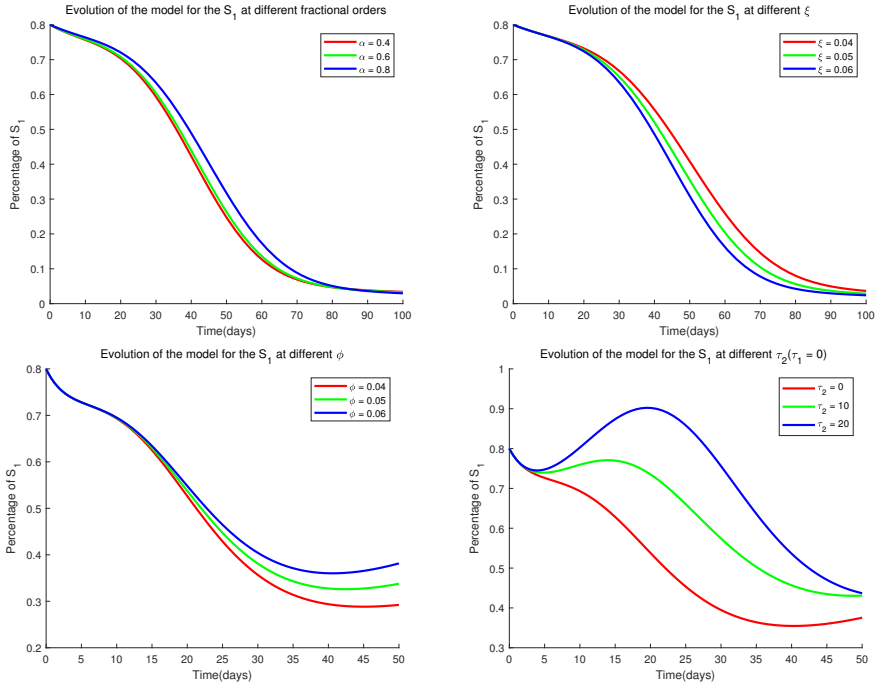

Figure 5. Evolution of unaware susceptible S_1 under varying: (a) fractional order $\alpha = 0.4$, 0.6, 0.8, (b) media impact $\xi = 0.004$, 0.005, 0.006, (c) media decay $\phi = 0.04$, 0.05, 0.06, (d) delay $\tau_2 = 0$, 10, 20 days.

Figure 6 displays the dynamics of asymptomatic infections A, symptomatic infections I, and unaware susceptible individuals S_1 under varying time delays τ_2. The results show that as τ_1 increases from 1 day to 20 days, the initial decay rate of A considerably slows down. Concurrently, longer delays lead to elevated levels of I and S_1. These patterns indicate that increased τ_1 delays intervention effectiveness, prolonging the transmission cycles of A and I while reducing the efficiency of transitioning S_1 into aware states.

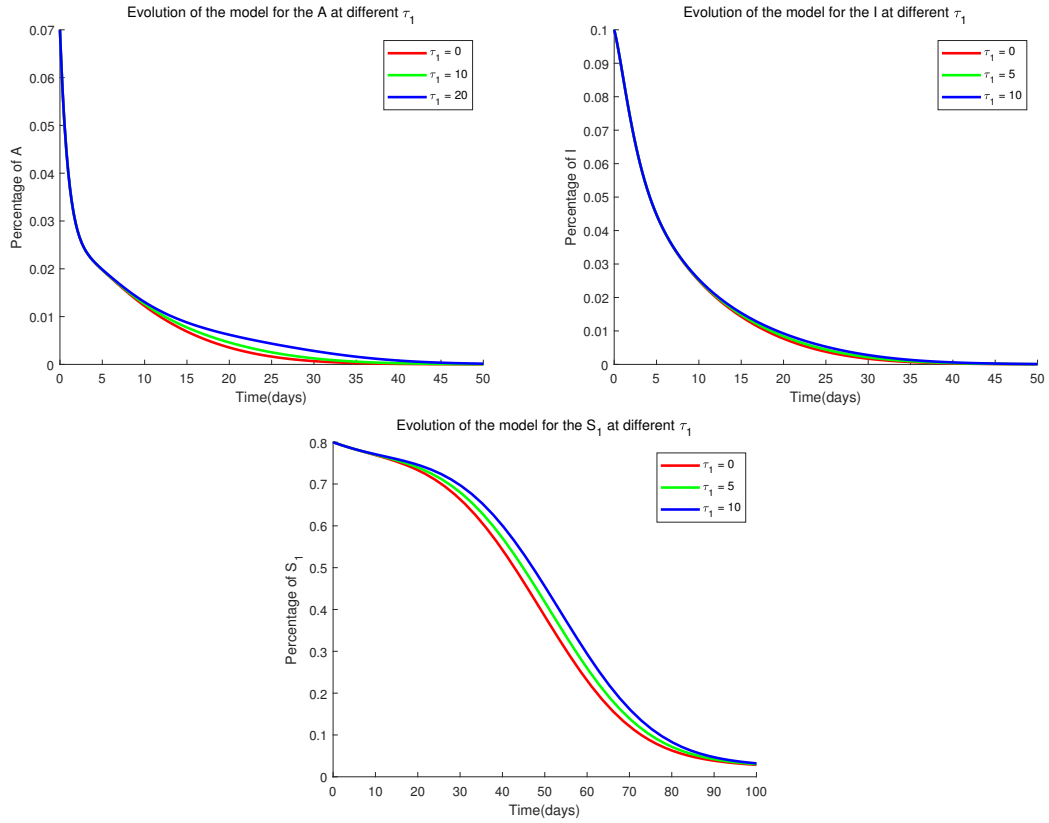

Figure 6. The system dynamics of asymptomatic infectors A, symptomatic infectors I, and unaware susceptibles S_1 under different time delays τ_2.

7.2. Optimal control numerical simulation and discussion

In addressing the optimal control problem for model (6.3), the solution procedure is implemented using the forward-backward sweep iterative method, with numerical computations performed via a fourth-order Runge-Kutta algorithm. Figure 7 compares the dynamics of asymptomatic infectors A, symptomatic infectors I, and unaware susceptibles S_1 under controlled and uncontrolled scenarios. The results demonstrate that the implementation of control measures leads to a marked reduction in infection prevalence and accelerates the convergence of the system to equilibrium. Moreover, the size of S_1 is effectively managed within the first 80 days under the optimal control strategy.

Although the objective function may also attain its minimum value without control, such a scenario corresponds to the maximum density of infected individuals. By contrast, infection density is minimized under the optimal control strategy, and the associated objective function value is lower than that under maximal control intensity. This finding implies that optimal control not only effectively suppresses infection density but also maintains intervention costs at their lowest feasible level. Consequently, an ideal balance is achieved between mitigating epidemic scale and optimizing resource allocation, providing a rigorous foundation for relevant decision-making.

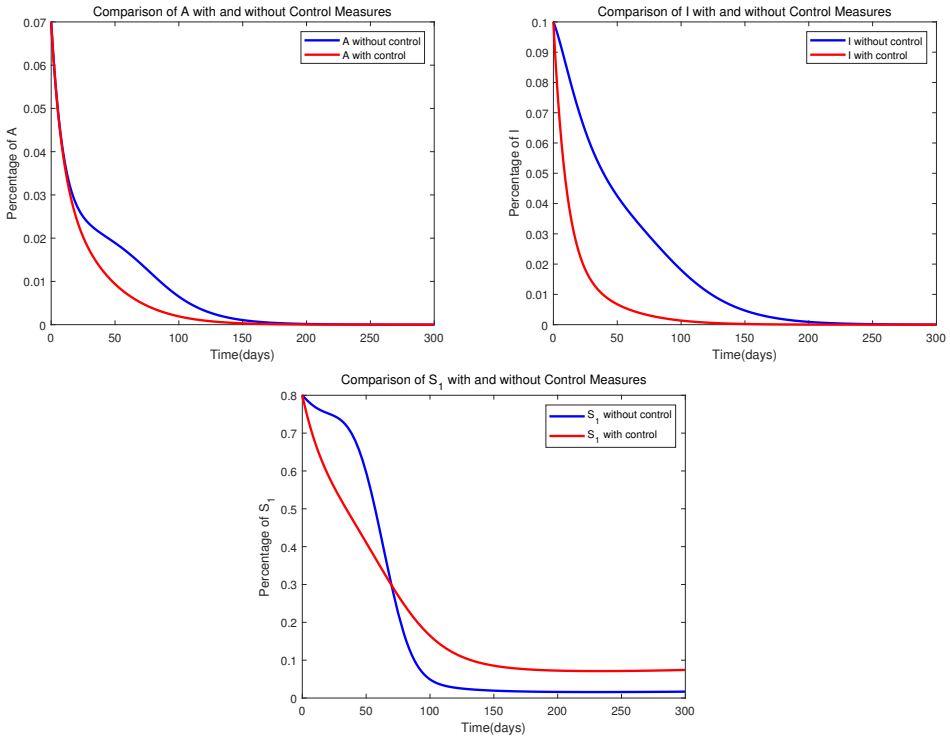

Figure 7. System dynamics in controlled and uncontrolled asymptomatically infected A, symptomatically infected I, and unawarely susceptible S_1 individuals.

8. Conclusions

This study presents the fractional-order SEAIQRM epidemic model that incorporates dual time delays, media effects, and vaccination-isolation control strategies. The framework stratifies susceptible individuals into aware and unaware classes, while integrating asymptomatic transmission, quarantine mechanisms, and media-related delays. The basic reproduction number R_0 is analytically derived, and the existence and uniqueness of the model solutions are rigorously established. A normalized forward sensitivity analysis identifies key parameters that influence R_0, leading to the selection of vaccination rate and isolation rate as control variables in the associated optimal control problem. Theoretical support for optimizing prevention and control strategies can be provided based on the theoretical optimality conditions. Numerical simulations confirm that combining strengthened isolation measures, active media communication, and public awareness initiatives with optimal control strategies leads to significant improvement in outbreak containment. The proposed model incorporates simplifying assumptions, particularly with regards to its limited capability to account for the spatial heterogeneity observed in real-world social systems. Moreover, the model considers direct inter-individual transmission as the primary route of infection, while not incorporating other complex pathways, such as indirect transmission. Future effort should prioritize the following: (1) constructing more biologically grounded disease models, (2) implementing network-based simulations that better capture real-world contact heterogeneity, and (3) incorporating additional contextual dimensions to improve the model's practical fidelity.

Author contributions

Wenli Huang: Writing – original draft, methodology. Ping Tong: Validation, supervision. Jing Zhang: Visualization. Qunjiao Zhang: Conceptualization. Jie Liu: review & editing. All authors have read and approved the final version of the manuscript for publication.

Use of Generative-AI tools declaration

The authors declare they have not used Artificial Intelligence (AI) tools in the creation of this article.

Acknowledgements

This research was supported by Natural Science Foundation of Hubei Province of China (2023AFB144).

Conflict of interest

All authors declare no conflicts of interest in this paper.

References

1. World Health Organization, World health statistics 2023: monitoring health for the SDGs, sustainable development goals. Available form: https://www.who.int/publications/i/item/9789240074323.
2. W. O. Kermack, A. G. McKendrick, A contribution to the mathematical theory of epidemics, *Proc. R. Soc. Lond. A*, **115** (1927), 700–721. https://doi.org/10.1098/rspa.1927.0118
3. M. El-Shahed, F. A. El-Naby, Fractional calculus model for childhood diseases and vaccines, *Appl. Math. Sci.*, **8** (2014), 4859–4866. https://doi.org/10.12988/ams.2014.4294
4. S. M. Salman, A. M. Yousef, On a fractional-order model for HBV infection with cure of infected cells, *J. Egypt. Math. Soc.*, **25** (2017), 445–451. https://doi.org/10.1016/j.joems.2017.06.003
5. I. Area, H. Batarfi, J. Losada, J. J. Nieto, W. Shammakh, Á. Torres, On a fractional order Ebola epidemic model, *Adv. Differ. Equ.*, **2015** (2015), 278. https://doi.org/10.1186/s13662-015-0613-5
6. T. Sardar, S. Rana, J. Chattopadhyay, A mathematical model of dengue transmission with memory, *Commun. Nonlinear Sci. Numer. Simul.*, **22** (2015), 511–525. https://doi.org/10.1016/j.cnsns.2014.08.009
7. L. Zhang, G. Huang, A. Liu, R. Fan, Stability analysis for a fractional HIV infection model with nonlinear incidence, *Discrete Dyn. Nat. Soc.*, **2015** (2015), 563127. https://doi.org/10.1155/2015/563127
8. R. Liu, J. Wu, H. Zhu, Media/psychological impact on multiple outbreaks of emerging infectious diseases, *Comput. Math. Methods Med.*, **8** (2007), 153–164. https://doi.org/10.1080/17486700701425870

9. G. Zaman, Y. H. Kang, I. H. Jung, Optimal treatment of an SIR epidemic model with time delay, *Biosyst*, **98** (2009), 43–50. https://doi.org/10.1016/j.biosystems.2009.05.006
10. C. C. McCluskey, Complete global stability for an SIR epidemic model with delay — Distributed or discrete, *Nonlinear Anal.*, **11** (2010), 55–59. https://doi.org/10.1016/j.nonrwa.2008.10.014
11. A. K. Misra, A. Sharma, V. Singh, Effect of awareness programs in controlling the prevalence of an epidemic with time delay, *J. Biol. Syst.*, **19** (2011), 389–402. https://doi.org/10.1142/S0218339011004020
12. C. Hsu, T. Yang, Existence, uniqueness, monotonicity and asymptotic behaviour of travelling waves for epidemic models, *Nonlinearity*, **26** (2012), 121. https://doi.org/10.1088/0951-7715/26/1/121
13. S. L. Wu, C. H. Hsu, Existence of entire solutions for delayed monostable epidemic models, *Trans. Am. Math. Soc.*, **368** (2016), 6033–6062. https://doi.org/10.1090/tran/6526
14. S. Kundu, S. Kouachi, S. Kumar, N. Kumari, Pattern formation and stability analysis in a delayed epidemic model with two aware classes, *Eur. Phys. J. Plus,* **139** (2024), 1079. https://doi.org/10.1140/epjp/s13360-024-05840-6
15. D. Greenhalgh, S. Rana, S. Samanta, T. Sardar, S. Bhattacharya, J. Chattopadhyay, Awareness programs control infectious disease – Multiple delay induced mathematical model, *Appl. Math. Comput.*, **251** (2015), 539–563. https://doi.org/10.1016/j.amc.2014.11.091
16. T. K. Kar, S. K. Nandi, S. Jana, M. Mandal, Stability and bifurcation analysis of an epidemic model with the effect of media, *Chaos Soliton. Fract.*, **120** (2019), 188–199. https://doi.org/10.1016/j.chaos.2019.01.025
17. K. A. Kabir, K. Kuga, J. Tanimoto, Analysis of SIR epidemic model with information spreading of awareness, *Chaos Soliton. Fract.*, **119** (2019), 118–125. https://doi.org/10.1016/j.chaos.2018.12.017
18. L. Feng, S. Jing, S. Hu, D. Wang, H. Huo, Modelling the effects of media coverage and quarantine on the COVID-19 infections in the UK, *Math. Biosci. Eng.*, **17** (2020), 3618–3636. https://doi.org/10.3934/mbe.2020204
19. T. Li, Y. Xiao, Complex dynamics of an epidemic model with saturated media coverage and recovery, *Nonlinear Dyn.*, **107** (2022), 2995–3023. https://doi.org/10.1007/s11071-021-07096-6
20. G. González-Parra, A. J. Arenas, B. M. Chen-Charpentier, A fractional order epidemic model for the simulation of outbreaks of influenza A(H1N1), *Math. Methods Appl. Sci.*, **37** (2014), 2218–2226. https://doi.org/10.1002/mma.2968
21. J. Singh, D. Kumar, Z. Hammouch, A. Atangana, A fractional epidemiological model for computer viruses pertaining to a new fractional derivative, *Appl. Math. Comput.*, **316** (2018), 504–515. https://doi.org/10.1016/j.amc.2017.08.048
22. N. Sene, SIR epidemic model with Mittag–Leffler fractional derivative, *Chaos Soliton. Fract.*, **137** (2020), 109833. https://doi.org/10.1016/j.chaos.2020.109833
23. Y. Chen, F. Liu, Q. Yu, T. Li, Review of fractional epidemic models, *Appl. Math. Model.*, **97** (2021), 281–307. https://doi.org/10.1016/j.apm.2021.03.044

24. D. Baleanu, M. Hassan Abadi, A. Jajarmi, K. Zarghami Vahid, J. J. Nieto, A new comparative study on the general fractional model of COVID-19 with isolation and quarantine effects, *Alex. Eng. J.*, **61** (2022), 4779–4791. https://doi.org/10.1016/j.aej.2021.10.030

25. C. Maji, Impact of media coverage on a fractional-order SIR epidemic model, *Int. J. Model. Simul. Sci. Comput.*, **13** (2022), 2250037. https://doi.org/10.1142/S1793962322500374

26. K. S. Nisar, M. Farman, M. Abdel-Aty, C. Ravichandran, A review of fractional order epidemic models for life sciences problems: past, present and future, *Alex. Eng. J.*, **95** (2024), 283–305. https://doi.org/10.1016/j.aej.2024.03.059

27. Y. H. Liang, K. J. Wang, Dynamics of the new exact wave solutions to the local fractional Vakhnenko–Parkes equation, *Fractals*, **25** (2025), 2550102. https://doi.org/10.1142/S0218348X25501026

28. K. J. Wang, The fractal active low-pass filter within the local fractional derivative on the Cantor set, *COMPEL*, **42** (2023), 1396–1407. https://doi.org/10.1108/COMPEL-09-2022-0326

29. X. Hao, S. Cheng, D. Wu, T. Wu, X. Lin, C. Wang, Reconstruction of the full transmission dynamics of COVID-19 in Wuhan, *Nature*, **584** (2020), 420–424. https://doi.org/10.1038/s41586-020-2554-8

30. Y. Zhang, R. Niu, Relaxation oscillations in an SIS epidemic model with a nonsmooth incidence, *Int. J. Bifurcat. Chaos*, **33** (2023), 2350188. https://doi.org/10.1142/S0218127423501882

31. X. Hao, L. Hu, L. Nie, Stability and global hopf bifurcation analysis of a schistosomiasis transmission model with multi-delays, *Int. J. Bifurcat. Chaos*, **35** (2025), 2550039. https://doi.org/10.1142/S0218127425500397

32. Z. Yu, J. Zhang, Y. Zhang, X. Cong, X. Li, A. M. Mostafa, Mathematical modeling and simulation for COVID-19 with mutant and quarantined strategy, *Chaos Soliton. Fract.*, **181** (2024), 114656. https://doi.org/10.1016/j.chaos.2024.114656

33. A. A. Kilbas, H. M. Srivastava, J. J. Trujillo, *Theory and applications of fractional differential equations*, North-Holland Mathematics Studies, Elsevier, 2006.

34. H. W. Berhe, O. D. Makinde, D. M. Theuri, Parameter estimation and sensitivity analysis of dysentery diarrhea epidemic model, *J. Appl. Math.*, **2019** (2019), 8465747. https://doi.org/10.1155/2019/8465747

35. W. Fleming, R. Rishel, *Deterministic and stochastic optimal control*, Stochastic Modelling and Applied Probability, New York: Springer, 1975. https://doi.org/10.1007/978-1-4612-6380-7

AIMS Press